

Precious Metals in the Holocene Sediments of the Chukchi Sea

N.V. Astakhova^a, , O.N. Kolesnik^a, A.S. Astakhov^a, X. Shi^b, L. Hu^c, A.V. Alatortsev^a

^a*V.I. Il'ichev Pacific Oceanological Institute, Far Eastern Branch of the Russian Academy of Sciences,
ul. Baltiiskaya 43, Vladivostok, 690041, Russia*

^b*First Institute of Oceanography, Ministry of Natural Resources, 6 Xianxialing Road, Laoshan District, Qingdao, 266061, China*

^c*Ocean University of China, 238 Songling Road, Laoshan District, Qingdao, 266100, China*

Received 4 April 2023; accepted 7 September 2023

Abstract—We studied the distribution of gold, silver, and platinum group elements (Pd, Pt, Rh, Ir, and Ru) in two bottom sediment cores of the southern Chukchi Sea. It is shown that the Holocene pelite–silty sediments with an age of up to 4.0 ka BP are significantly enriched in these elements, except for Ru and Rh, relative to their clarkes. Native silver minerals were found in all samples by probe microanalysis, whereas gold minerals were revealed only in the surface layer of the sediment core closest to the Chukchi Sea coast. Multicomponent statistical analysis of the chemical composition and grain size of the sediments and the content of organic matter in them has led to the conclusion about the accumulation of clastogenic and chemogenic forms of precious metals. The abnormally high content of gold (0.3 ppm) in the recent sediments near the Chukchi Peninsula coast might be due to its additional removal from the continent as a result of the placer mining there.

Keywords: gold; silver; PGE; Holocene deposits; Chukchi Sea

INTRODUCTION

The contents and distribution of gold and other precious metals (PM) in the bottom sediments of the Chukchi Sea shelf have been studied by many researchers (Ainemer et al., 1984; Ivanova and Kreiter, 2006; Astakhov et al., 2010; Nesterenko et al., 2014; Kolesnik et al., 2018), because primary and placer deposits of gold and silver of alluvial, alluvial–proluvial, alluvial–marine, and coastal–marine genesis with an Eocene–Holocene age are widespread on the Chukchi Peninsula and Alaska coasts (Buryak, 2003). There are both gold placers and clusters of fine-grained gold in sands of the coastal Chukchi Sea shelf (Gol'dfarb, 2009; Nesterenko et al., 2014). Chemical analysis of samples of silty, mainly diatomaceous, sediments from the deep-water areas of the South Chukchi plain (Fig. 1) showed local abnormal contents of PM (Astakhov et al., 2010; Nesterenko et al., 2014). Probe microanalysis (Kolesnik et al., 2018) revealed single gold, silver, and platinum grains.

Therefore, there are different viewpoints of the genesis and sources of gold and other PM in the bottom sediments of the southern Chukchi Sea. The shelf is promising for flooded alluvial and littoral placers, including placers of fine-grained gold (Ainemer et al., 1984; Tsar'kova et al.,

1993; Gol'dfarb, 2009). In addition, the possibility of chemogenic or biochemical accumulation of PM in the organic-carbon-enriched silts of the South Chukchi Plain is considered (Gol'dfarb, 2009; Astakhov et al., 2010, 2013). A similar mechanism is assumed for the present-day Bering Sea environment (Pashkova et al., 1988; Anikiev et al., 1997) and is taken into account by many researchers of ancient carbonaceous deposits (Yudovich and Ketris, 1988; Buryak, 2003).

Unfortunately, the available information about PM on the Chukchi Sea shelf is concerned only with their distribution in the surface layer of bottom sediments, which is not insufficient for understanding the role of biogeochemical processes in their accumulation and redistribution. Therefore, the goal of this work was to study the distribution of PM in the Holocene silty sediments of the southern Chukchi Sea depending on their age, the content of organic carbon in them, and the activity of biogeochemical processes and to elucidate the sources of PM and the factors that govern the accumulation of these metals. The study was performed in two cores (Fig. 1) of Holocene sediments: from an area with a high content of organic matter in the sediments and with known mineralogical and geochemical anomalies of PM (core LV77-4) and from the site where a high intensity of biogeochemical processes was earlier established (Matveeva et al., 2015) (core LV77-1).

Although both stations are located on the shelf within the South Chukchi Plain, they are in the zones of the predominance of waters of the Siberian coastal (LV77-1) and Pacific

 Corresponding author.

E-mail address: n_astakhova@poi.dvo.ru (N.V. Astakhova)

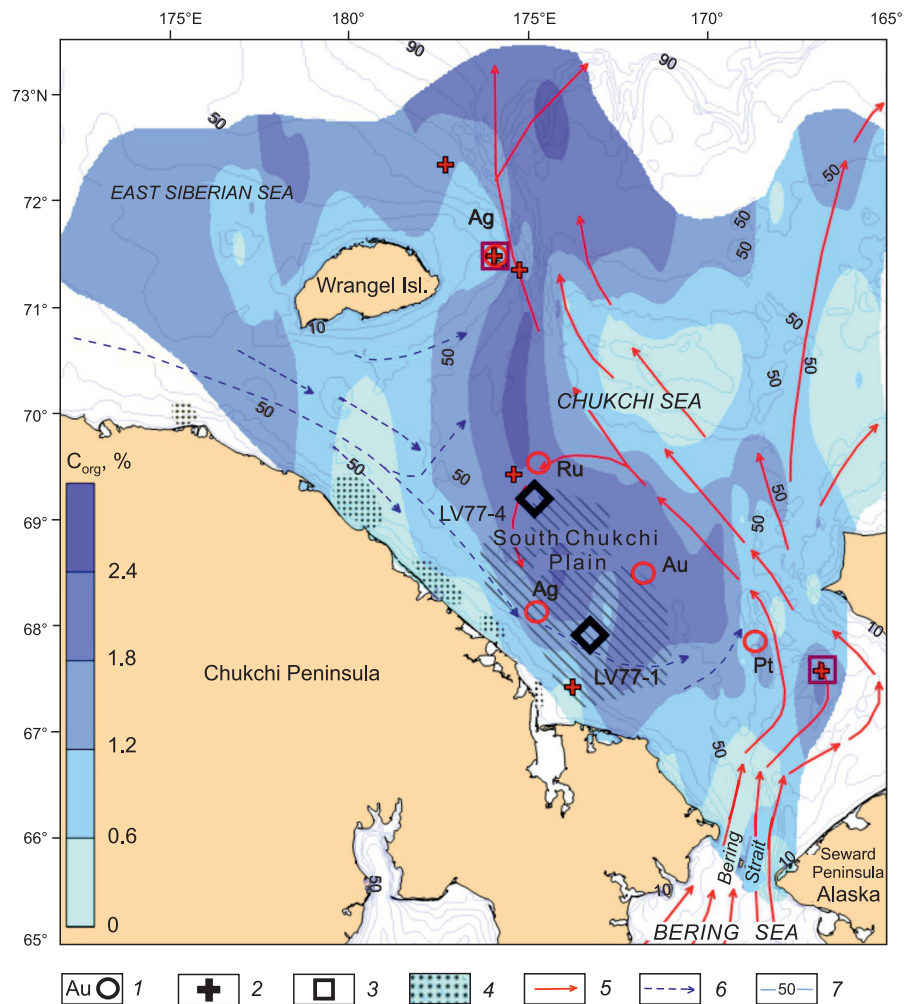


Fig. 1. Location of the studied cores, C_{org} content in the Chukchi Sea surface sediments (Astakhov et al., 2013), and geochemical and mineralogical anomalies of precious metals. 1 – geochemical anomalies of precious metals in the bottom sediments (Astakhov et al., 2013); 2, 3 – findings of native-metal minerals (Kolesnik et al., 2018): 2 – gold, 3 – platinum; 4 – shelf zones with revealed gold placers (Gol'dfarb, 2009); 5, 6 – spread of: 5 – Pacific waters, 6 – waters of the Siberian coastal current; 7 – depth contours (m). Oblique shading marks the zone with a low oxygen content (<6 ml/L) in the bottom waters in summer (Frolov, 2008).

(LV77-4) currents (Fig. 1). The Pacific waters arrive at the Chukchi Sea via the Bering Strait, with an extreme velocity of up to 150 cm/s in its eastern part. This current carries a large amount of sedimentary (including biogenic) material, estimated at 110–154 mln tons/year (with a water turbidity of 5–7 g/m³) (Lisitsyn, 1966). Having left the strait, the Pacific current turns first to the northeast, into Kotzebue Bay, and then separates into streams. The main stream runs to the northwest, curving round the South Chukchi Plain in the north (Fig. 1). The cold and denser waters of the East Siberian Sea flow from the Long Strait along the Chukchi Peninsula coast. The current jets in the central zone of the basin form a chalistase, where they bring a large amount of terrigenous and biogenic suspended material. Under calm hydrodynamic conditions, sedimentation of fine-grained material and steady long-term accumulation of sediments take place in the inner zone of this chalistase (Pavlidis, 1982). In the central zone of the Chukchi Sea shelf, primary diagenesis

in the surface layer of clayey silts proceeds under reducing conditions (Logvinenko and Ogorodnikov, 1980). These conditions are due to the water stagnation inside the chalistase, aggravated by the long-standing (nine or more months a year) sea ice cover (Pavlidis, 1982).

MATERIALS AND METHODS

The bottom sediment cores for study were sampled with a gravity tube during the 77th cruise of the R/V Akademik Lavrentiev in the southern Chukchi Sea in 2016 (Fig. 1, Table 1). At the same points, the partly studied (Li et al., 2020; Vologina et al., 2023) surface sediment horizon (30–40 cm) was sampled with a multicorer. At the point of sampling of the core LV77-1, two cores were taken and studied in 2012: A 34 cm thick core b28, cut with a box corer (Astakhov et al., 2018), and a 110 cm thick core HC-11, taken with a hydrostatic tube (Matveeva et al., 2015; Tsoy et al., 2017).

Table 1. Results of radiocarbon dating of cores

Station, N, W, sea depth	Sampling interval, cm	Material	Laboratory	¹⁴ C AMS age, yr BP
LV77-1, 67°52.019', 172°37.563', 44 m	72–73	Semidecomposed shell fragment	NSKA-01761	2350 ± 82
	101–102	Large shell fragment	NSKA-01762	2902 ± 100
	258	Shell fragment	Beta-478640	3580 ± 30
	313	<i>Macoma</i> sp. shell	Beta-478641	4110 ± 30
LV77-4, 69°13.055', 174°51.890', 49 m	308	Large <i>Macoma</i> sp. shell fragment	Beta-478644	3890 ± 30
	321	Shell fragment	NSKA-1777	4141 ± 79

The age of sediments was determined by the AMS¹⁴C method in different laboratories (Table 1). The ¹⁴C dates of the samples were calibrated against the Marine13 calibration curve (Reimer et al., 2009) to obtain their calendar age; the ΔR value was taken equal to 360 ± 135 yr BP. The rate of sedimentation in the surface sediment layer was determined from the ²¹⁰Pb and ¹³⁷Cs contents (Astakhov et al., 2018; Li et al., 2020; Vologina et al., 2023). The chemical composition of sediments was determined by X-ray fluorescence scanning of the wet cores at 3 mm intervals, using an XRF spectrometer with an Olympus Delta DPO-2000 XRF analyzer. The data obtained were used to demonstrate the distribution of some elements throughout the core via variations in the ratios of their contents to the Rb content (Alartortsev et al., 2023; Kolesnik et al., 2023a).

Core for analysis for PM was sampled at 10 cm intervals. The samples were ground to a fraction smaller than 0.063 mm in an agate mortar; then, their weighed specimens were used for analysis for PM and for a general chemical analysis. The contents of PM were determined on an Elan 9000 ICP mass spectrometer at the Yu.A. Kosygin Institute of Tectonics and Geophysics (ITG) FEB RAS, Khabarovsk, by the standard technique with precipitation of tellurium (Jin and Zhu, 2000). The ground sample was fused with sodium peroxide (Na₂O₂). The alloy was dissolved in acidified hot water and evaporated to remove silica by its insolubilization. Gold and PGE were preconcentrated and separated from numerous matrix elements by coprecipitation with Te. The detection limits of elements were as follows (ppb): Ru, Rh, and Ir – 1, Pd and Au – 7, and Pt – 9 (10⁻¹⁰⁰%) (Jin and Zhu, 2000).

Organic carbon (C_{org}) and biogenic carbonates in the same samples were determined by the IR detection method on a Shimadzu TOC-V total organic carbon analyzer (Japan) at the Analytical Center of the Far East Geological Institute (AC FEGI) FEB RAS, Vladivostok. The content of the total carbon (TC) was determined by burning a ca. 50 mg dry sample in a flow of high-purity (99.995%) oxygen at 905 °C. The content of inorganic carbon (IC) was evaluated by acidifying the sample with phosphoric acid and its calcination at 200 °C. The C_{org} content was determined from the difference between the contents of total and inorganic carbon. The relative standard deviations of the contents of total and inorganic carbon were 1.5 and 2.0%, respectively. The total chemical composition of the samples was studied by

their acid digestion at the AC FEGI FEB RAS. The silicon content was determined by gravimetry, and the contents of the other major elements, by ICP MS on an iCAP 6500Duo (Thermo Scientific Corporation, USA) spectrometer. The contents of trace elements were measured by ICP MS on an Agilent 7700x (Agilent Technologies, USA) spectrometer. The grain sizes of the samples were determined by a standard technique on an Analysette 22 NanoTec analyzer. Following the international classification (Wentworth, 1922), we have identified pelite (<4 μm), silt (4–65 μm), and sand (>65 μm) fractions.

The presence of PM minerals and pyrite (a potential accumulator of PM) in the sediments was assessed from the results of probe microanalysis, which was carried out by a proven technique (Kolesnik et al., 2018) on a JEOL JXA-8100 microprobe with an Oxford INCA Energy energy-dispersive attachment at the AC FEGI FEB RAS. We used one background sample (LV77-1 (110–120 cm thick)) and four samples with a high gold content determined by ICP MS. Using the water–sieve method, we separated sand (>63 μm) and silt (4–63 μm) fractions in each sample. For analysis, these fractions were glued onto a 20 × 12 mm conductive contact tape and sprayed with a thin carbon layer.

Statistical and graphical processing of the analytical results was performed using the EXCEL and STATISTI-CA-10 standard software.

RESULTS

Composition of sediments and PM distribution in the core LV77-1. The core LV77-1 was sampled in the halystatic area of the South Chukchi Plain (Fig. 1), in the zone of the predominant influence of the waters of the Siberian coastal current. The core sediments are homogeneous olive-gray or greenish-gray pelitic silts. Silt amounts to 79.8–84.6%; pelite, 15.2–20.2%; and sand, 0.003–0.3%. Higher contents of sand and silt are observed in the upper part of the core, and pelite is more abundant in its lower part (Fig. 2, Table 2). Many horizons of the sedimentary core contain variably preserved shells and shell detritus. Some of the found shell fragments were dated (Table 1); their maximum age is 3.7 ka BP, with regard to the uneven sedimentation rate (Fig. 2). The upper part of the core is completely identical in dates and composition to the sediments at the same

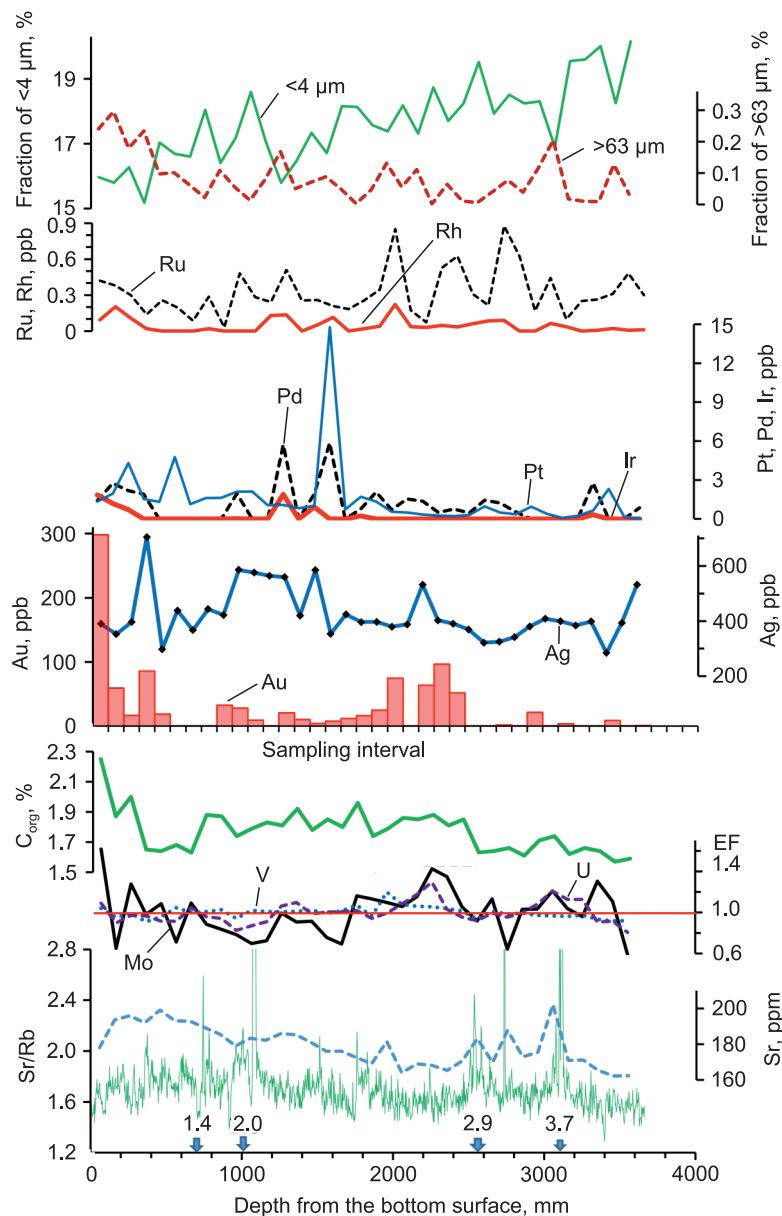


Fig. 2. Contents of precious metals and compositional specifics of Holocene deposits in the core LV77-1. Arrows mark the points of radiocarbon dating and the age of sediments (ka BP). The contents of PM are given in Table 2. Sampling interval is 10 cm. The contents of Sr as an indicator of bioproductivity and the contents of Mo, V, U, and Al, used to calculate the enrichment factors according to Scholz et al. (2017), were determined in the samples by AAS. The Sr/Rb values were obtained by X-ray fluorescence scanning at 3 mm intervals and indicate the presence of mollusk shells.

point of the earlier studied core NS-11 (Tsoy et al., 2017), which permits comparison of the two cores and using the earlier obtained data on diatoms, methane content, and organic-carbon characteristics (Matveeva et al., 2015; Tsoy et al., 2017).

The sediments of the surface layer (36 cm thick) were referred to as biogenic–terrigenous according to their mineral composition (Vologina et al., 2023). The biogenic part is diatom relics and single sponge spicules and mollusk shells. For mineralogical analysis, we used the fraction of 0.05–0.25 mm, which was divided into heavy and light ones. The

heavy fraction in the sediment samples amounts to 0.24–0.59%. The light fraction is dominated by quartz, plagioclase, and feldspars; biotite and muscovite are subordinate. Almost all samples contain volcanic glass, carbonates, mica–clay aggregates, and rock fragments. There are also minor coal, carbonized plant remains, diatom valves, and sponge spicules. The heavy fraction comprises minerals of epidote, garnet, amphibole, and pyroxene groups, ilmenite, magnetite, sphene, leucoxene, and goethite. There are also minor chloritoid, brookite, hematite, apatite, tourmaline, zircon, and carbonates. Some samples contain sillimanite, chromian

Table 2. Contents of precious metals ($10^{-7}\%$) and C_{org} (%) and granulometric composition (%) of sediments in the core LV77-1

Interval, cm	Ru	Rh	Pd	Ir	Pt	Au	Ag	C_{org}	Pel	Sl	Sd
5	0.42	0.09	1.40	1.85	1.34	298.22	390.28	2.30	15.97	83.79	0.24
15	0.38	0.20	2.76	1.20	1.97	59.45	352.67	1.90	15.79	83.91	0.30
25	0.30	0.11	2.18	0.71	4.31	16.82	396.72	2.00	16.27	83.55	0.18
35	0.14	0.02	1.91	0.00	1.54	85.92	704.60	1.70	15.18	84.58	0.23
45	0.26	0.00	0.00	0.00	1.31	18.68	298.05	1.60	17.03	82.87	0.10
55	0.20	0.00	0.00	0.00	4.78	0.00	438.27	1.70	16.69	83.20	0.10
65	0.09	0.00	0.00	0.00	1.14	0.00	367.10	1.60	16.60	83.34	0.06
75	0.29	0.02	0.00	0.00	1.62	0.00	443.42	1.90	18.04	81.94	0.02
85	0.03	0.00	0.00	0.00	1.64	32.59	421.65	1.90	16.41	83.49	0.11
95	0.48	0.00	1.95	0.01	2.10	28.26	585.78	1.70	17.18	82.76	0.06
105	0.28	0.00	0.00	0.00	2.11	8.94	575.51	1.80	18.59	81.39	0.01
115	0.24	0.13	0.00	0.00	1.07	0.00	564.28	1.80	17.05	82.86	0.08
125	0.51	0.14	5.72	1.89	1.09	20.42	559.03	1.80	15.80	84.03	0.17
135	0.26	0.00	0.00	0.00	0.84	10.32	420.06	1.90	16.46	83.49	0.05
145	0.26	0.05	1.91	0.91	1.03	3.99	585.32	1.80	17.33	82.60	0.07
155	0.21	0.11	5.85	0.00	14.77	7.59	353.74	1.90	16.71	83.20	0.09
165	0.18	0.00	0.00	0.00	0.74	11.87	424.17	1.80	18.16	81.80	0.05
175	0.26	0.02	0.76	0.24	1.72	16.14	395.95	2.00	18.14	81.86	0.00
185	0.35	0.04	2.07	0.00	1.33	24.98	397.13	1.70	17.57	82.38	0.05
195	0.85	0.22	0.73	0.00	0.55	74.76	379.78	1.80	17.38	82.48	0.13
205	0.17	0.04	1.53	0.00	0.49	0.00	388.00	1.90	18.18	81.77	0.06
215	0.07	0.03	1.37	0.00	0.35	63.72	531.90	1.90	17.31	82.58	0.11
225	0.53	0.05	0.50	0.00	0.27	96.22	402.71	1.90	18.73	81.26	0.00
235	0.63	0.03	0.77	0.00	0.23	51.87	390.48	1.80	17.71	82.23	0.06
245	0.31	0.06	0.46	0.00	0.30	0.00	369.42	1.90	18.24	81.74	0.01
255	0.22	0.08	1.44	0.00	0.96	0.00	321.62	1.60	19.52	80.48	0.01
265	0.88	0.09	1.22	0.00	0.50	1.68	324.80	1.60	17.93	82.03	0.04
275	0.62	0.00	0.54	0.00	0.36	0.00	341.51	1.70	18.51	81.41	0.08
285	0.17	0.00	0.00	0.00	0.94	21.30	380.69	1.60	18.24	81.72	0.04
295	0.44	0.06	0.00	0.00	0.41	0.00	408.42	1.70	18.30	81.58	0.11
305	0.10	0.04	0.00	0.00	0.10	3.72	399.43	1.70	16.89	82.90	0.20
315	0.25	0.00	0.00	0.00	0.25	0.00	384.37	1.60	19.55	80.43	0.02
325	0.26	0.01	2.78	0.34	0.65	0.00	398.33	1.70	19.61	80.38	0.01
335	0.31	0.02	0.03	0.00	2.32	8.62	284.62	1.60	20.01	79.98	0.01
345	0.48	0.01	0.00	0.00	0.18	0.00	393.45	1.60	18.25	81.62	0.13
355	0.30	0.01	0.85	0.00	0.00	0.95	531.74	1.60	20.16	79.81	0.03

Note. Hereafter, bold-typed are the contents of elements higher than their clarkes. Pel – pelite, Sl – silt, Sd – sand.

spinel, staurolite, and rutile. The homogeneous lithologic composition of sediments testifies to a stable depositional environment during their formation (Vologina et al., 2023).

The chemical composition of sediments throughout the core section is nearly homogeneous. The contents of major elements in the sediments vary slightly: The standard deviation of the content from its median value varies from 0.00 for Mg to 0.34 for Si. Trace elements show a more intricate distribution: The standard deviation of their contents varies from 0.1 to 0.8; for Li, V, Cr, Ni, Cu, Zn, As, Rb, Sr, Zr, Ba, and Pb, it is within 1.0–28.7. Nevertheless, the contents of

elements, except for Si, Na, and As, do not exceed their clarkes in argillaceous shales (Sklyarov, 2001).

For some trace elements (Mo, V, and U) being indicators of anoxic conditions, we calculated the enrichment factor (EF), i.e., the ratio of their aluminum-normalized content in the sample (Me/Al) to their regional lithogenic background content ($(Me/Al)_{bgr}$) (Scholz et al., 2017):

$$Me_{EF} = (Me/Al)/(Me/Al)_{bgr}$$

The EF was determined as the average value over the core: Mo – $0.355 \cdot 10^{-4}$, V – $18.256 \cdot 10^{-4}$, and U – $0.389 \cdot 10^{-4}$.

The calculated EF value for Mo in the studied core samples is close to that in the entire Chukchi Sea surface bottom sediments, $0.338 \cdot 10^{-4}$ (Astakhov et al., 2015).

The contents of PM and organic carbon and the granulometric composition of the core sediments are presented in Table 2. The C_{org} content varies from 1.6 to 2.3%. Higher C_{org} contents are found in the upper part of the core (Fig. 2). The contents of silver are higher than its clarke (Sklyarov, 2001) throughout the 335 cm thick sediment core (its accumulation coefficient (K_a) reaches 9.65). Elevated contents of gold ($K_a \leq 85.21$) are observed in most of the core sediment samples. Platinum ($K_a \leq 2.59$) and iridium ($K_a \leq 2.84$) enrich only a few sediment layers (Table 2). Figure 2 shows correlations of the gold content with the C_{org} content and the K_a values for Mo, V, and U. One can see that the gold content is most significantly correlated with the C_{org} content (correlation coefficient r is 0.62) and with the K_a value for Mo ($r = 0.55$). The coefficients of correlation between the gold

content and the K_a values for V and U are insignificant but positive.

Composition of sediments and PM distribution in the core LV77-4. The 315 cm thick bottom sediment core LV77-4 was sampled in the central part of the South Chukchi Sea basin (Fig. 1), in the zone of the Pacific waters and accumulation of sediments enriched in diatoms and organic carbon (Astakhov et al., 2015). The sediments are black, dark gray, olive-gray, or greenish-gray homogeneous pelitic silts with lighter spots and lenses (Kolesnik et al., 2023a). The sediment often contains remains of semidecomposed shells. Silt amounts to 79.4–84.1%; pelite, 15.3–20.5%; and sand, 0.004–0.9%. Higher contents of sand and silt are observed in the upper part of the core, and pelite is most abundant in the lower part (Fig. 3, Table 3).

The contents of PM and organic carbon and the granulometric composition of the core sediments are presented in Table 3. The contents of gold are higher than its clarke

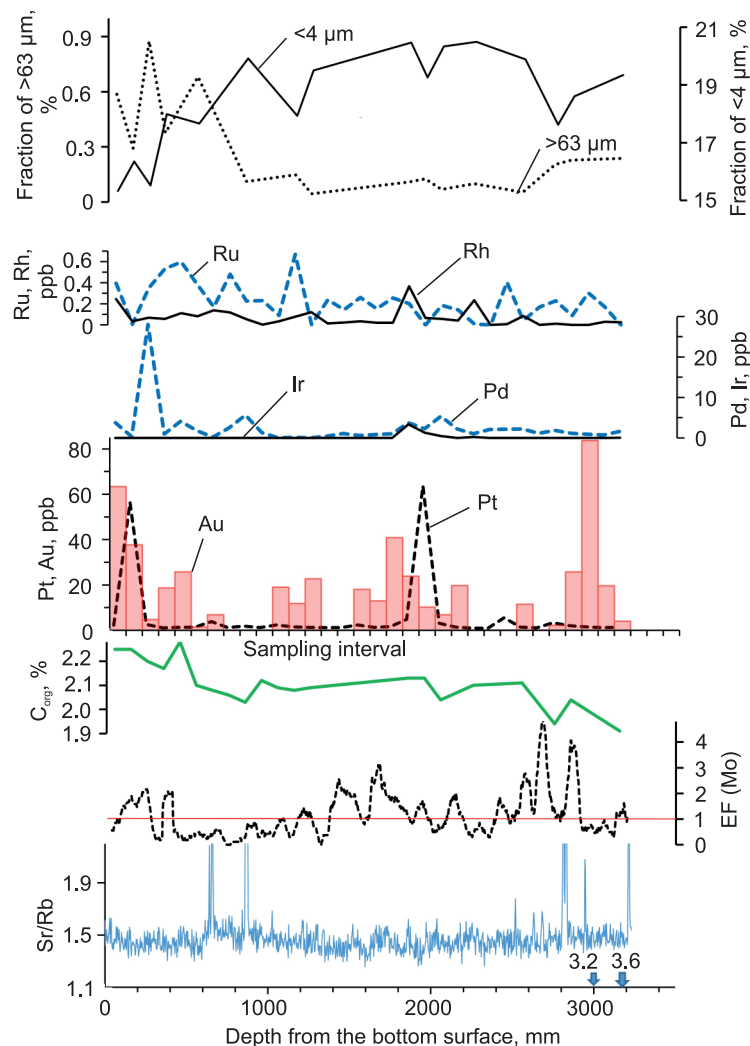


Fig. 3. Contents of precious metals and compositional specifics of Holocene deposits in the core LV77-4. Arrows mark the points of radiocarbon dating and the age of sediments (ka BP). The contents of PM are given in Table 3. Sampling interval is 10 cm. The enrichment factors for Mo and the Sr/Rb values were obtained by X-ray fluorescence scanning at 3 mm intervals and testify to fluctuations in the redox conditions of the bottom water (EF) and the presence of mollusk shells (Sr/Rb).

Table 3. Contents of precious metals (10^{-7} %) and C_{org} (%) and granulometric composition of sediments (%) in the core LV77-4

Interval, cm	Ru	Rh	Pd	Ir	Pt	Au	C_{org}	Pel	Sl	Sd
5	0.39	0.25	3.76	0.00	1.82	63.41	2.25	15.33	84.08	0.59
15	0.01	0.03	0.33	0.00	53.86	37.72	2.25	16.35	83.36	0.29
25	0.35	0.07	28.03	0.00	2.13	4.73	2.20	15.51	83.61	0.87
35	0.53	0.06	0.96	0.00	0.71	18.70	2.17	17.99	81.64	0.38
45	0.60	0.11	4.12	0.00	0.97	25.74	2.28	17.66	81.65	0.68
55	0.38	0.08	1.77	0.00	0.99	1.46	2.10	N.a.	N.a.	N.a.
65	0.17	0.14	0.17	0.00	3.38	6.83	2.08	N.a.	N.a.	N.a.
75	0.48	0.12	2.52	0.00	0.81	0.00	2.06	N.a.	N.a.	N.a.
85	0.23	0.05	5.64	0.00	1.46	0.00	2.03	19.91	79.97	0.11
95	0.23	0.00	1.33	0.00	0.85	0.00	2.12	N.a.	N.a.	N.a.
105	0.09	0.03	0.00	0.00	1.92	19.03	2.09	N.a.	N.a.	N.a.
115	0.67	0.08	0.15	0.00	1.10	11.83	2.08	17.93	81.92	0.15
125	0.00	0.12	0.00	0.00	0.92	22.70	2.09	19.50	80.45	0.04
135	0.24	0.02	0.41	0.00	0.87	0.00	N.a.	N.a.	N.a.	N.a.
145	0.14	0.02	1.06	0.00	0.84	0.00	N.a.	N.a.	N.a.	N.a.
155	0.26	0.04	0.61	0.00	1.96	18.05	N.a.	N.a.	N.a.	N.a.
165	0.15	0.02	0.83	0.00	0.97	12.96	N.a.	N.a.	N.a.	N.a.
175	0.26	0.02	1.03	0.00	1.20	40.88	N.a.	N.a.	N.a.	N.a.
185	0.20	0.37	3.76	3.33	4.23	23.91	2.13	20.47	79.42	0.11
195	0.00	0.07	2.28	1.29	60.80	10.20	2.13	19.26	80.61	0.13
205	0.19	0.06	5.34	0.43	2.61	6.90	2.04	20.33	79.60	0.07
215	0.14	0.04	2.21	0.00	1.02	19.75	N.a.	N.a.	N.a.	N.a.
225	0.01	0.23	1.03	0.20	0.61	0.00	2.10	20.49	79.41	0.10
235	0.00	0.00	2.07	0.00	0.49	0.00	N.a.	N.a.	N.a.	N.a.
245	0.41	0.01	2.14	0.00	5.00	0.00	N.a.	N.a.	N.a.	N.a.
255	0.04	0.08	2.22	0.00	1.06	11.54	2.11	19.88	80.06	0.05
265	0.17	0.00	1.14	0.00	0.77	0.00	N.a.	N.a.	N.a.	N.a.
275	0.23	0.01	1.85	0.00	2.82	2.23	1.94	17.62	82.17	0.20
285	0.09	0.00	1.16	0.00	1.62	25.73	2.04	18.60	81.17	0.23
295	0.30	0.00	0.89	0.00	1.16	83.63	N.a.	N.a.	N.a.	N.a.
305	0.17	0.03	0.73	0.00	0.78	19.65	N.a.	N.a.	N.a.	N.a.
315	0.00	0.03	1.60	0.05	0.90	3.97	1.91	19.34	80.42	0.24

Note. N.a. – not analyzed.

(Sklyarov, 2001) in most of the sediment samples ($K_a \leq 23.89$). Platinum ($K_a \leq 10.67$), palladium ($K_a \leq 3.11$), and iridium ($K_a \leq 5.12$) enrich only a few sediment layers (Table 3). Moreover, the contents of Pt, Ir, and Pd are higher and the content of Au is lower than those in the core LV77-1. There is no visible correlation between the PM contents and the granulometric composition of sediments (Fig. 3). At the same time, there is a correlation between the gold content and the EF values for Mo, determined by the above formula but from the results of X-ray fluorescence scanning at 3 mm intervals (Fig. 3).

PM minerals. To determine the PM species in the sediments, we took four samples from the core intervals with a high gold content (core LV77-1: intervals 0–10, 40–50, and 190–200 cm; core LV77-4: interval 290–300 cm) and one background sample with a minimum gold content (core

LV77-1: interval 110–120 cm). The preparations were examined under a scanning electron microscope (SEM) equipped with an electron microprobe. The probe microanalysis revealed PM minerals in the sediments of the cores LV77-1 and LV77-4. These are scarce fine grains of different shapes, no larger than 4–5 μm (Fig. 4a, b). Minerals were detected in both the sand and silt fractions. The maximum number of mineral grains (14 silver grains) was found in the sand fraction of sediment from the core LV77-1 (interval 110–120 cm). Chemical analysis of all grains showed that silver is present in the sediments mostly as oxides and less as sulfates (Fig. 5). In the upper 10 cm of the core LV77-1, we found oxygen compounds of silver and gold with significant amounts of copper, zinc, and mercury (Au–Ag–Cu–Zn–O, Au–Cu–Zn–O, Ag–Hg–O, and Ag–O). Copper and zinc are permanent impurities in the PM minerals; often, uranium,

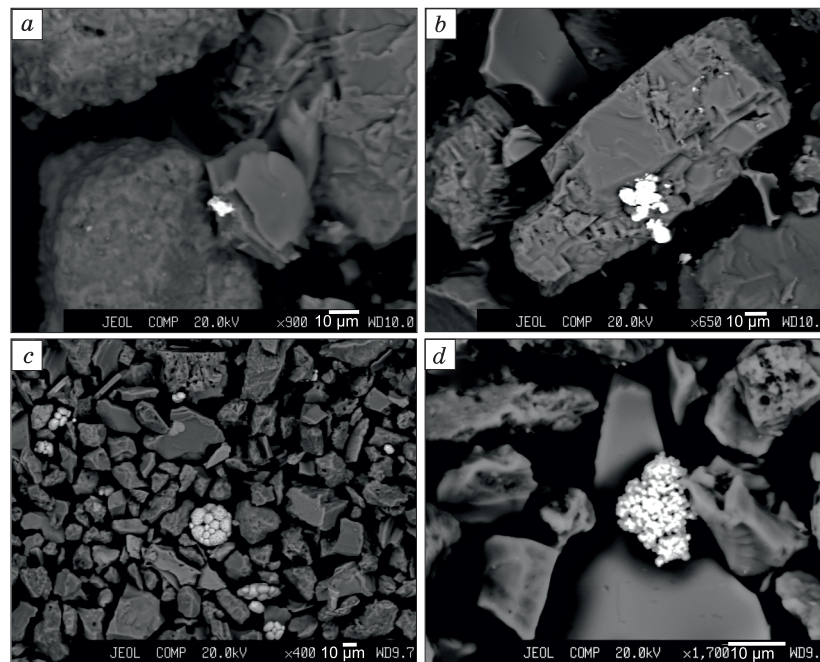


Fig. 4. Morphology of PM minerals and pyrite (white and light gray segregations) in the sediments of the core LV77-1-1, Chukchi Sea (BSE images): *a, b* – silver oxides at the surface of K-feldspar, interval 110–120 cm, fraction of >63 μm ; *c, d* – framboid pyrite among rock-forming minerals, interval 190–200 cm, fraction of 4–63 μm .

and, sometimes, thorium, tellurium, sulfur, and chlorine are also present (Fig. 5).

In addition to PM, the sediments contain much framboidal pyrite of different degrees of aggregation (Fig. 4*c, d*). The aggregates reach $50 \times 50 \mu\text{m}$ in size ($d = 70 \mu\text{m}$). To assess the abundance of pyrite in the sediments, we compared the maps of sulfur and iron distribution obtained by scanning of a given site of the sample at a specified magnification (fraction of > 63 μm , $\times 60$; fraction of 4–63 μm , $\times 95$). We calculated the scanning area (S_{scan}), the area of overlapping of S and Fe (SFe-S, mm^2), and its percentage of the scanning area (SFe-S, %). The more detailed study of the core LV77-1 showed the minimum amount of pyrite in the form of single fine grains in the upper 10 cm of the sediment section. In the underlying horizons, pyrite is more abundant, and the degree of aggregation of its grains increases. In the sand fraction, the maximum content of pyrite is found in the interval 110–120 cm (SFe-S = 0.0684%), and in the silt fraction, in the interval 190–200 cm (SFe-S = 1.5860%). The average SFe-S value in the sand and silt fractions over the two cores is 0.0406 and 0.5174%, respectively. It is obvious that the silt fraction is the main carrier of pyrite in the sediments.

DISCUSSION

Common trends in PM distribution. The primary analysis of PM contents in the studied cores (Tables 2 and 3, Figs. 2 and 3) revealed uneven distribution of Pt, Pd, and Ir throughout the section and their enrichment of sediments in

the core LV77-4 sampled in the zone of the Pacific waters. The maximum contents of Pt, Pd, and Ir in this core are 60.8, 28.0, and 3.33 ppm, respectively, whereas in the core LV77-1 they are 14.8, 5.7, and 1.89 ppm. In the surface layer of sediments, platinum and palladium grains were also found (Kolesnik et al., 2018) in the zone of the Pacific waters (Fig. 1). The contents of Pt, Pd, and Ir in both cores are at the clark level, except for a few abnormal peak values (Tables 2 and 3). There is no obvious trend in the distribution of other PGE (Rh and Ru); their contents do not exceed their clarkes. Platinum group elements in the silty sediments of the Chukchi Sea might be supplied from the Dime Creek platinum placers on the eastern coast of the Bering Strait (western coast of the Seward Peninsula) (Kutyrev et al., 2020).

The distribution of silver was studied only in the core LV77-1. Although all samples are characterized by high contents of Ag ($K_a = 3.9\text{--}9.7$), it shows different distribution trends. The presence of sulfate minerals and weakly oxidized native-silver grains with Au, Cu, Zn, and Hg impurities (Fig. 5) suggests its both allothigenic and authigenic accumulation. In both cores, except for the upper 10 cm of the core LV77-1, gold is present in background contents from 0 to 80–90 ppb (Tables 2 and 3, Figs. 2 and 3), which show periodic variations. Assuming a regular rate of sedimentation in the core LV77-4 (Fig. 3) and interpolating the dates in the core LV77-1 (Fig. 2), we estimate this periodicity at approximately a thousand years. Such cyclicity is typical of variations in total solar insolation at this latitude (Darby et al., 2012). This parameter governs the erosion and removal of material from land and the shelf processes (ice coverage, bioproductivity, water stratification). Both cores

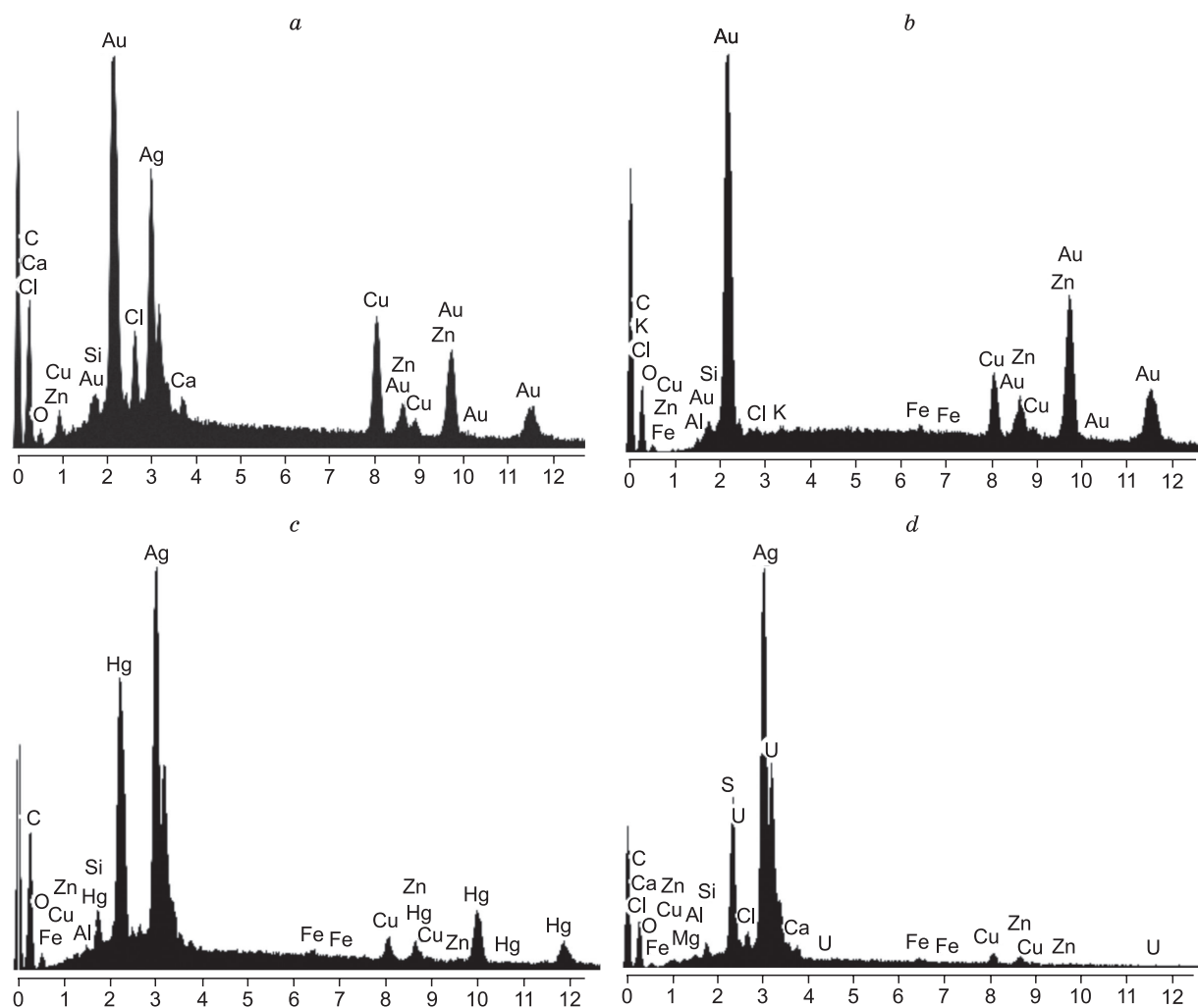


Fig. 5. Energy-dispersive X-ray spectra of PM minerals in the Chukchi Sea sediment sections (abscissa axis marks energy, keV; ordinate axis marks peak intensity): *a* – oxygen compound of Au and Ag with a significant content of Cu and Zn and a Cl impurity; *b* – oxygen compound of Au with Cu and Zn; *c* – oxygen compound of Ag and Hg with Cu and Zn impurities; *d* – silver sulfate with Cu, Zn, and U impurities.

were sampled in the zone where bottom waters are depleted in oxygen in summer (Fig. 1) because of its consumption for the oxidation of accumulating organic matter (Frolov, 2008). In addition, the high gold contents in the cores are correlated with the high C_{org} contents and K_a values of Mo, V, and U, which is an indicator of anoxic depositional environment (Kholodov and Nedumov, 2005; Scholz et al., 2017).

It is necessary to study the ways of PM accumulation and the role of organic matter in it in more detail. Applying modern analytical methods for determining trace contents of PM (gold and PGE), researchers from different countries determined the concentrations of these elements in sea and ocean waters and their transfer and accumulation in sediments. Precious metals are supplied into seawater both as dissolved and partly hydrolyzed species and as finely dispersed (including nanosize) particles. Experimental studies showed that dissolved metals form stable complexes with oxygen-containing organic ligands and are also concentrated by living matter (biogenic concentration). This ensures

the concentration and migration of PM in organomineral compounds and their deposition during sedimentogenesis (Goldberg and Koide, 1990; Kizil'shtein, 2000; Varshall et al., 2000; Kubrakova et al., 2017, 2022). The decomposition of organic matter under the action of microorganisms begins already in the upper layers of sediment at the earliest stages of diagenesis (Tissot and Welte, 1978).

The possibility of anthropogenic gold enrichment. The sediment samples from the upper 10 cm of the core LV77-1 have an abnormal gold content (0.3 ppm) and a maximum C_{org} content (Fig. 2). This gold enrichment is observed only in the core located closer to the coast, in the zone of transfer of continental sedimentary material by the Siberian coastal current (Fig. 1). Since this is the only sample with native gold (Fig. 5), we assume an additional supply of continental gold from the Chukchi Peninsula, where gold placers were mined in the 20th century. In addition to fine-grained gold (not trapped during gold mining) and organomineral compounds, ancient organic matter of Quaternary deposits can be

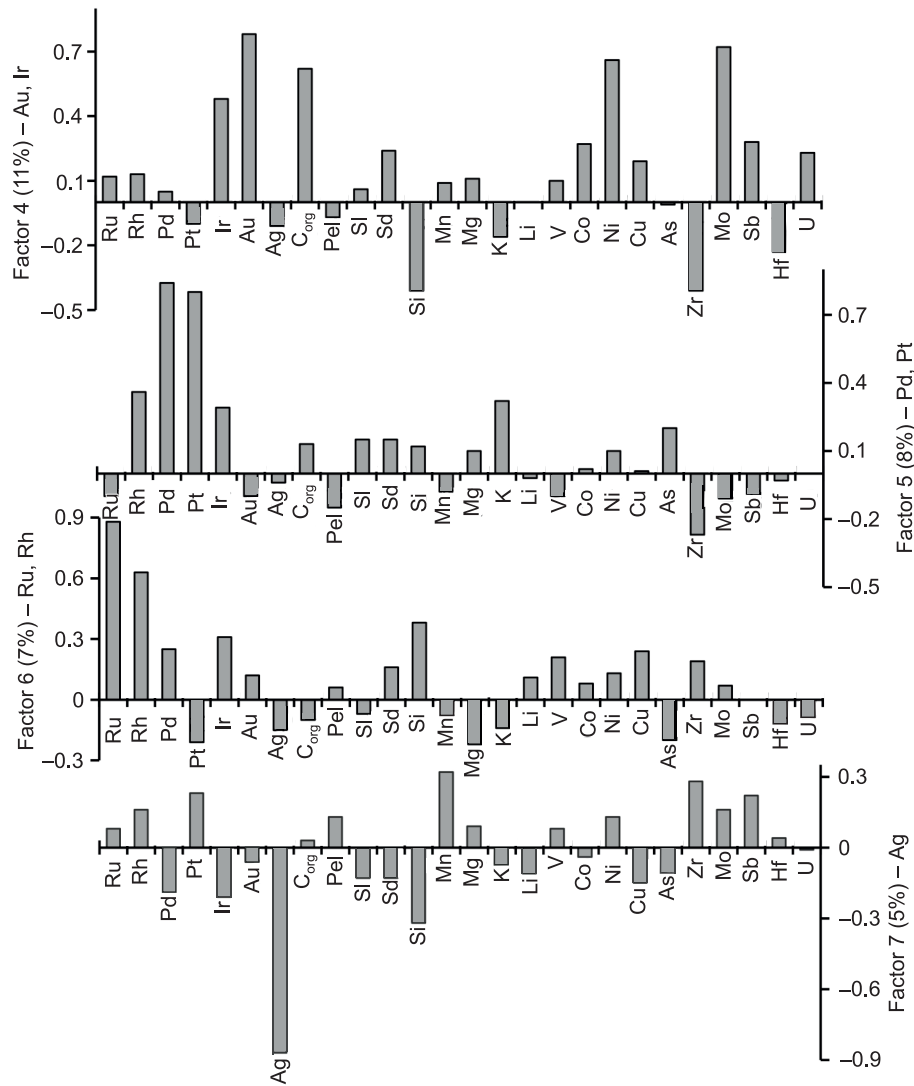


Fig. 6. Contributions of factors 4–7 to the sampling variability (the total contribution is 31%), determined by chemical elements and other parameters (Sd – sand, SI – silt, and Pel – pelite) in the sediment core LV77-1.

removed and accumulate in the sediments. According to the determined rate of sedimentation at this point (0.43 mm/year) (Astakhov et al., 2018), the upper 10 cm of the sediments accumulated for 220 years, which rules out an anthropogenic impact on the lower sediment horizons.

Statistical analysis of PM distribution. To establish the relationships among the contents of PM, major and trace elements, and C_{org} and the granulometric composition of sediments in the core LV77-1, we performed a correlation analysis of the parameters. It showed a significant positive correlation of PM only with granulometric fractions, C_{org} , and some trace elements (Mo, Ni, and Cu). All PM, except for Ru, are negatively correlated with the pelite fraction and positively correlated with the sand or silt fraction.

For a sampling of 36 samples and 26 varying parameters, including PM, granulometric fractions, C_{org} , and chemical elements showing a significant positive or negative correlation with PM ($> \pm 0.2$), we performed an *R*-factor analysis to

identify the factors that determine the contribution of individual parameters or their groups to the variability of this sampling (Fig. 6). Factor 1 providing 17% of the sampling variability is determined by variations in the granulometric composition of sediments. Factors 3 and 4, yielding 16 and 12% of the sampling variability, are determined by variations in the contents of groups of elements accumulating in the finest-grained fractions (Hf, Co, U, Sb, Li, and Mn) and in the components (feldspars and carbonates) of the silt fractions of sediment (V, Cu, K, Mg, and C_{org}).

The PM determining factors 4–7 yield a total of 31% of the sampling variability. The contribution of different PM to these factors and their correlation with other varying parameters are shown in Fig. 6. Silver (factor 7), in contrast to PGE and gold, makes a negative contribution to the sampling variability, which indicates other sources or modes of its accumulation in the sediments. In factor 7, Ag is associated with the sand and silt fractions and with Si (Fig. 6),

which is a typical element of these fractions (Astakhov et al., 2013). Probably, Ag accumulates in the sediments mainly together with coarse-clastic terrigenous components, but we cannot substantiate this simple mechanism because of the diversity of Ag species.

Factors 5 and 6, providing 8 and 7% of the sampling variability, respectively, are determined by variations in the contents of Ru, Rh, Pt, and Pd (Fig. 6). These PGE are associated with the coarse sand (Ru, Rh) and sand–silt (Pt, Pd) fractions of sediments and with chemical elements specific to these fractions. In factor 6, PGE are grouped with Si and Zr, and in factor 5, Ru and Rh are grouped with K typical of feldspars accumulating in silt fractions.

The most intricate interpretation of factor loadings is for factor 4: The contents of Au and Ir are also associated with the content of sand but are not associated with the contents of Si, K, and Zr typical of clastic sand fractions. This suggests that Au and Ir are associated with pyrite, a crucial component of the fraction of 4–63 μm . They are also strongly correlated with C_{org} and elements accumulating together with it under anoxic conditions (Mo, V, U, and, less, Ni) and with elements adsorbed by authigenic pyrites (Sb, Cu, Ni, and Co) (Astakhova and Razzhigaeva, 1988). This is partly consistent with the established periodicity of gold accumulation and with the correlation of the gold content with the EF values for Mo, U, and V (Fig. 2).

Precious metals and organic matter. The results of the factor analysis for the core LV77-1 (Fig. 6) and the distribution of PM in the cores (Figs. 2 and 3) indicate at least three processes of gold accumulation/concentration in the silt deposits of the South Chukchi Plain: concentration as a result of hydraulic differentiation of fine-grained gold carried from land; biochemical accumulation of dissolved gold carried from land or contained in organomineral compounds; concentration in the above two ways as a result of the intense removal of gold from land during the gold placer mining. To estimate the probability of these processes, we performed correlation and factor analyses for the cores LV77-1 and LV77-4, using samplings including only PM, granulometric fractions, and C_{org} (36 and 32 samples, 11 and 9 varying parameters, respectively) (Fig. 7a, c) and ignoring the upper two samples most enriched in C_{org} , with possible anthropogenic “pollution” (Fig. 7b, d).

Based on the results of correlation (Table 4) and *R*-factor analyses (Fig. 7) of the complete samplings for the cores LV77-1 and LV77-4 (36 and 32 samples, respectively), we have identified multielement association II (Fig. 7a, c) including Au and C_{org} , which are steadily grouped with coarse granulometric fractions. In the core LV77-4, this association comprises Au, C_{org} , and silt and sand fractions (Fig. 7c), and in the core LV77-1, it comprises Au, C_{org} , and Ir (Fig. 7a). In the core LV77-1, silver is found only in coarse granulo-

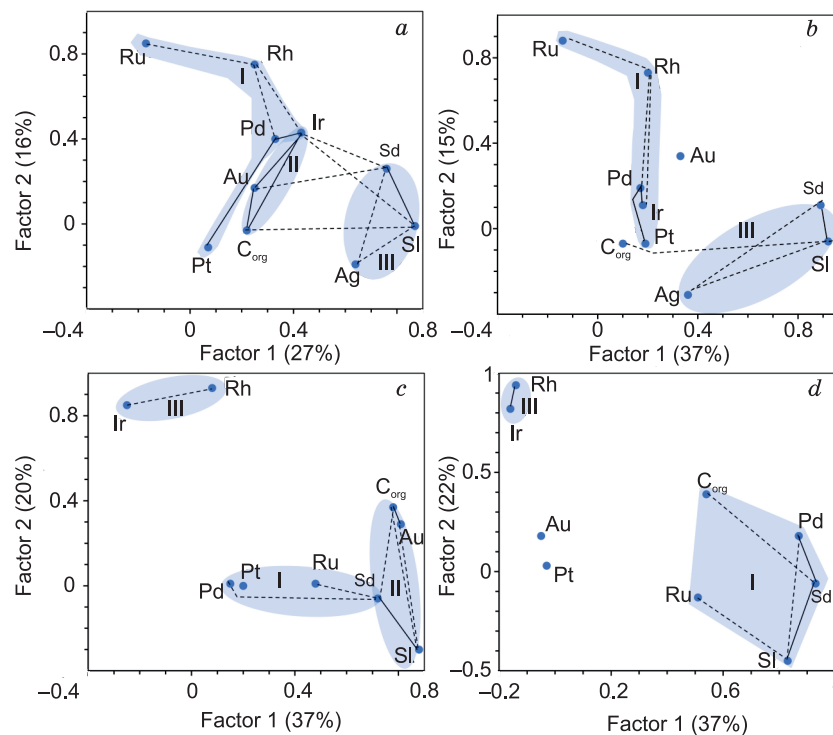


Fig. 7. Factor 1–factor 2 diagrams reflecting the relationship of PM with granulometric fractions (Sd – sand, Sl – silt) and organic carbon (C_{org}) in the sediment cores LV77-1 (a, b) and LV77-4 (c, d). a, c – All samples ($n = 36$ and 32), b, d – without samples from the upper 20 cm of the sediment ($n = 34$ and 30). Gray shading and Latin numbers indicate multielement associations, solid lines mark the strongest positive correlations, and dashed lines show other significant positive connections. The pelite fraction is omitted, because it has the value of factor 1 from -0.8 to -0.9 in all diagrams and shows no significant correlations with other variable parameters.

Table 4. Correlation matrices of chemical elements in the sediments from the stations LV77-1 and LV77-4

<i>a</i>											<i>b</i>											
Ele- ment	Ru	Rh	Pd	Ir	Pt	Au	Ag	Pel	Sl	Sd	Ele- ment	Ru	Rh	Pd	Ir	Pt	Au	Ag	Pel	Sl	Sd	
Ru	1										Ru	1										
Rh	0.43	1									Rh	0.46	1									
Pd	0.10	0.47	1								Pd	0.09	0.44	1								
Ir	0.14	0.47	0.54	1							Ir	0.10	0.35	0.62	1							
Pt	-0.18	0.20	0.54	0.01	1						Pt	-0.18	0.21	0.55	0.01	1						
Au	0.17	0.26	0.10	0.53	-0.05	1					Au	0.19	0.20	0.08	-0.05	-0.09	1					
Ag	-0.19	-0.09	0.17	0.13	-0.08	0.06	1				Ag	-0.18	-0.02	0.20	0.30	-0.08	0.29	1				
Pl	0.10	-0.34	-0.33	-0.44	-0.27	-0.37	-0.30	1			Pl	0.15	-0.22	-0.29	-0.30	-0.28	-0.30	-0.37	1			
A	-0.11	0.32	0.32	0.42	0.27	0.36	0.30	-1.00	1		A	-0.15	0.22	0.29	0.30	0.28	0.29	0.37	-1.00	1		
S	0.01	0.48	0.30	0.56	0.09	0.49	0.17	-0.76	0.73	1	S	-0.06	0.29	0.24	0.29	0.11	0.28	0.34	-0.73	0.71	1	
C _{org}	-0.04	0.32	0.22	0.51	0.20	0.62	0.07	-0.43	0.43	0.32	C _{org}	-0.12	0.25	0.22	0.21	0.25	0.25	0.16	-0.34	0.35	0.05	

<i>c</i>											<i>d</i>										
Ele- ment	Ru	Rh	Pd	Ir	Pt	Au	Pel	Sl	Sd	Ele- ment	Ru	Rh	Pd	Ir	Pt	Au	Pel	Sl	Sd		
Ru	1									Ru	1										
Rh	0.06	1								Rh	-0.07	1									
Pd	0.19	-0.03	1							Pd	0.16	-0.05	1								
Ir	-0.14	0.66	-0.03	1						Ir	-0.16	0.76	-0.05	1							
Pt	-0.37	-0.18	-0.13	0.19	1					Pt	-0.28	-0.06	-0.06	0.33	1						
Au	0.18	0.35	-0.19	0.03	0.15	1				Au	0.23	0.23	-0.25	0.28	-0.05	1					
Pl	-0.44	0.17	-0.41	0.40	-0.14	-0.54	1			Pl	-0.58	0.43	-0.60	0.39	0.08	-0.05	1		-		
A	0.42	-0.19	0.35	-0.40	0.17	0.55	-1.00	1		A	0.57	-0.47	0.55	-0.41	-0.06	0.03	-0.99	1			
S	0.52	-0.02	0.67	-0.26	-0.10	0.34	-0.81	0.75	1	S	0.52	-0.17	0.73	-0.23	-0.14	0.11	-0.84	0.77	1		
C _{org}	0.36	0.35	0.23	0.04	0.28	0.63	-0.53	0.50	0.59	C _{org}	0.47	0.35	0.34	0.14	0.11	0.48	-0.31	0.25	0.56		

Note. *a*, *b* – Core LV77-1: *a* – all samples ($n = 36$), *b* – without samples from the upper 20 cm ($n = 34$); *c*, *d* – core LV77-4: *c* – all samples ($n = 33$), *d* – without samples from the upper 20 cm ($n = 31$). Bold-typed are the significant values of correlation coefficient.

metric fractions and forms a single association with them, III (Fig. 7a). In both cores, PGE are worse correlated with coarse sediment fractions than Au and Ag and form one (Fig. 7a) or two multielement associations (Fig. 7c). In the core LV77-1, Ir is associated both with other PGE and with the Au–C_{org} group and is a component of both association II and association I (Fig. 7a). In addition, it is well correlated with coarse granulometric fractions. In the core LV77-4, Ir and Re form association III and are better correlated with the pelite fraction than with the sand and silt ones. Iridium is characterized by a negative value of factor 1 (Fig. 7b, c) and a weak positive correlation with pelite.

In the samplings for the cores LV77-1 and LV77-4, which exclude the upper 20 cm of the sediment (Fig. 7b, d), the identified associations of PGE and Ag are generally preserved, but association II (Au–C_{org}–Ir–silt–sand) disappears. Positive correlations between these elements remained but became insignificant (Table 4b, c). In the core LV77-4, the association of gold and C_{org} with coarse fractions is significantly weaker, judging from the values of factor 1 (Fig. 7c). Thus, the exclusion of two surface sediment samples with

possible anthropogenic “pollution” from the data set indicates that the natural distribution of gold depends little on the granulometric composition of sediments and their C_{org} content. In the surface layer of sediments, gold is very intimately associated with C_{org} because of its biogeochemical accumulation by the latter or their joint accumulation as a result of their intense removal from land during the placer mining.

The joint accumulation of Au and C_{org} is more likely for the core LV77-1 sampled in the near-continental zone of transfer of suspended material carried from the land (Fig. 1). The core LV77-4 is far from the land and is located in the zone of the Pacific waters, which carry a large amount of biogenic material (resulting from an intense bloom of phytoplankton) from the northern part of the Bering Sea into the Chukchi Sea (Pavlidis, 1982). Therefore, it is worth considering the possibility of gold accumulation as organomineral compounds or finely dispersed metallic inclusions in the organic matter of biogenic remains, with their subsequent release or redistribution during early diagenesis. Earlier, fine inclusions of native Au (0.4–3.1 μm) and Ag (1.8–8.3 μm) were found in the wood and plant remains buried in

Pleistocene sediments in the Chukchi Sea (Goryachev et al., 2020). The presence of organomineral gold compounds in organic matter and the possibility of their transport together with it are widely discussed for the present-day and ancient deposits (Pashkova et al., 1988; Kizil'shtein, 2000; Kubrakova et al., 2017).

All PM are positively correlated with organic carbon to varying degrees of significance. Significant correlations of C_{org} with Au ($r = 0.62$) and Ir ($r = 0.51$) in the core LV77-1 (Table 4a) and with Au ($r = 0.63$) in the core LV77-1 (Table 4c) are observed only in the top layer of the cores, which suggests that these elements accumulated in organic compounds during sedimentogenesis. The weaker correlations between them in the lower parts of the cores might be due to the decomposition of deposited organic matter by microorganisms, which begins at the moment of its burial during early diagenesis. This process is accompanied by the removal of metals from the organic matter and their migration (Goldberg and Koide, 1990; Colodner et al., 1992). Model sorption experiments showed that dissolved PM species are concentrated on geochemical barriers, mainly on iron oxides and oxyhydroxides (Kubrakova et al., 2011, 2012, 2017), which can serve as collectors of inorganic PM species.

During the subsequent action of sulfate-reducing bacteria under anaerobic conditions, iron oxides of the sediments transform to produce authigenic pyrite, which contains microimpurities of various metals, including Ag (analysis for Au and PGE was not carried out) (Astakhova and Razzhigaeva, 1988; Kolesnik et al., 2023b).

The cyclicity of gold accumulation observed in the cores LV77-1 and LV77-4 calls for additional study in terms of changes in the depositional environments, variability of currents, and abrasion and erosion runoff from the coasts. Analysis of changes in the accumulation of organic matter seems the most promising because of variations in the ice covering and bioproductivity and hydrochemistry of the bottom waters. At present, there are anoxic conditions in the study area (Fig. 1), which favor the accumulation of C_{org} .

The results of the statistical analysis and the mineral composition of the samples suggest that PM are present in the Holocene sediments in two forms, clastogenic and chemogenic. Clastogenic silver was found almost in the entire core LV77-1, and gold, only in the upper layer of sediments. Earlier, grains of PM (Ag, Au, Pt, Pd–Pt) and compounds Au–Cu–Ag, Cu–Zn–Ag, and Cu–Ag were found in the surface layer of the Chukchi Sea sediments at several stations (Kolesnik et al., 2018). The wide spread of gold and silver placers in the littoral zone of the southern Chukchi Sea suggests that they are the source of these metals and arrive with the Siberian coastal water current at the South Chukchi Basin. Probably, PGE are removed by the Pacific current from the Dime Creek platinum placer in the Bering Strait area (western coast of the Seward Peninsula) and, possibly, from the platinum placers of the Goodnews Bay area in southwestern Alaska (Kutyrev et al., 2020).

CONCLUSIONS

The performed studies showed a significant gold and silver enrichment (relative to the Au and Ag clarkes) of fine-grained silty sediments with an age of up to 4 ka BP in the southern Chukchi Sea. The contents of PGE (Pd, Pt, Rh, Ir, and Ru) are lower than their clarkes, except for some samples. Higher gold contents were found near the Chukchi Sea coast, in the zone with a predominance of the Siberian coastal water current. Higher PGE contents were detected in the zone of the Pacific waters removing sedimentary material from the coast of Alaska, where PGE placers are localized. The probe microanalysis of the core sediments revealed native silver minerals in all samples, whereas gold minerals were found only in the surface layer of the sediment core closest to the Chukchi Sea coast.

All elements show a positive correlation with the contents of organic carbon and the silt–sand fractions of sediments. Gold is also correlated with redox-sensitive elements of anoxic environments (Mo, V, and U) and demonstrates periodic accumulation synchronously with them (every thousand years). The results of the statistical analysis of the contents of major and trace elements, PM, organic matter, and granulometric fractions suggest the accumulation of both clastogenic and chemogenic forms of PM. We assume that much gold accumulates in the chemogenic (biogeochemical) form, with a transition of its organomineral compounds into sulfide ones during the early diagenesis of sediments.

The abnormally high content of gold (0.3 ppm) in the surface sediments near the Chukchi Sea coast might be due to its additional supply from the continent during the placer mining there.

ACKNOWLEDGEMENTS AND FUNDING

We thank the captain, crew, and members of the research team of the 77th cruise of the R/V Akademik M.A. Lavrentiev for assistance during the expedition, as well as N.V. Berdnikov and A.A. Karabtsov for assistance with analyses.

The research was financially supported by grant 21-17-00081 from the Russian Science Foundation. The expedition work was financially supported by project 121021700342-9 from the Ministry of Science and Higher Education of the Russian Federation and by Grant No. 2018SDKJ0104-3 from the Shandong Province of China for the National Laboratory for Marine Science and Technology (Qingdao).

REFERENCES

- Ainemer, A.I., Egiazarov, B.Kh., Krasnov, S.G., Likht, F.R., 1984. The problem of metal-bearing sediments and fine-grained gold, in: Problems of Marine Mineral Resources [in Russian]. DVNTs AN SSSR, Vladivostok, pp. 93–103.
- Alatortsev, A.V., Kolesnik, A.N., Shi, X., Hu, L., Karnaukh, V.N., Astakhov, A.S., 2023. Lithological and geochemical indicators of

- ice gouging: Evidences from Holocene sediments in the East Siberian Sea. *Russ. Geol. Geophys.* 64 (9), 1040–1047, doi: [10.2113/RGG20234528](https://doi.org/10.2113/RGG20234528).
- Anikiev, V.V., Dudarev, O.V., Kolesov, G.M., Sapozhnikov, D.Yu., Bot-sul, A.I., 1997. Effect of lithodynamic factors on noble-metal distribution in particulate matter and bottom sediments in the marine part of the Anadyr Estuary. *Geochem. Int.* 35 (5), 467–482.
- Astakhov, A.S., Kolesov, G.M., Dudarev, O.V., Ivanov, M.V., Kolesnik, A.N., 2010. Noble metals in the bottom sediments of the Chukchi Sea. *Geochem. Int.* 48, 1208–1219, doi: [10.1134/S0016702910120050](https://doi.org/10.1134/S0016702910120050).
- Astakhov, A.S., Kolesnik, A.N., Shakirov, R.B., Gusev, E.A., 2013. Conditions of the accumulation of organic matter and metals in the bottom sediments of the Chukchi Sea. *Russ. Geol. Geophys.* 54 (9), 1056–1070, doi: [10.1016/j.rgg.2013.07.019](https://doi.org/10.1016/j.rgg.2013.07.019).
- Astakhov, A.S., Bosin, A.A., Kolesnik, A.N., Obrezkova, M.S., 2015. Sediment geochemistry and diatom distribution in the Chukchi Sea: Application for bioproductivity and paleoceanography. *Oceanography* 28, 190–201, doi: [10.5670/oceanog.2015.65](https://doi.org/10.5670/oceanog.2015.65).
- Astakhov, A.S., Vologina, E.G., Dar'in, A.V., Kalugin, I.A., Plotnikov, V.V., 2018. Influence of global climate changes in past centuries on the chemical composition of bottom sediments in the Chukchi Sea. *Russ. Meteorol. Hydrol.* 43, 251–257, doi: [10.3103/S1068373918040064](https://doi.org/10.3103/S1068373918040064).
- Astakhova, N.V., Razzhigaeva, N.G., 1988. Crystal morphology and contents of trace elements in pyrite from Far Eastern marine sediments. *Tikhookeanskaya Geologiya*, No. 6, 103–108.
- Buryak, V.A., 2003. The Fundamentals of Gold Minerogeny [in Russian]. *Dal'nauka*, Vladivostok.
- Colodner, D.C., Boyle, E.A., Edmond, J.M., Thomson, J., 1992. Post-depositional mobility of platinum, iridium and rhenium in marine sediments. *Nature* 358, 402–404, doi: [10.1038/358402a0](https://doi.org/10.1038/358402a0).
- Darby, D.A., Ortiz, J.D., Grosch, C.E., Lund S.P., 2012. 1,500-year cycle in the Arctic Oscillation identified in Holocene Arctic sea-ice drift. *Nat. Geosci.* 5, 897–900, doi: [10.1038/ngeo1629](https://doi.org/10.1038/ngeo1629).
- Frolov, I.E. (Ed.), 2008. Review of Hydrometeorological Processes in the Arctic Ocean 2007 [in Russian]. AANII, St. Petersburg.
- Gol'dfarb, Yu.I., 2009. Dynamics of Formation, Classification, and Age of Alluvial Gold Placers in Northeastern Asia. DSci Thesis [in Russian]. SVKNII DVO RAN, Magadan.
- Goldberg, E.D., Koide, M., 1990. Understanding the marine chemistries of the platinum group metals. *Mar. Chem.* 30, 249–257, doi: [10.1016/0304-4203\(90\)90074-M](https://doi.org/10.1016/0304-4203(90)90074-M).
- Goryachev, N.A., Sotskaya, O.T., Astakhov, A.S., Shi Xuefa, Mikhailitsyna, T.I., Aksentov, K.I., Berdnikov, N.V., 2020. Ore mineralization in Pleistocene sediments of Long Strait (East Siberian Sea). *Dokl. Earth Sci.* 491, 220–223, doi: [10.1134/S1028334X20040066](https://doi.org/10.1134/S1028334X20040066).
- Ivanova, A.M., Kreiter, E.N., 2006. Small- and fine-grained gold in shelf areas of the World Ocean. *Geologiya i Poleznye Iskopaemye Mirovogo Okeana*, No. 2, 30–49.
- Jin, X., Zhu, H., 2000. Determination of platinum-group elements and gold in geological samples with ICP-MS using sodium peroxide fusion and tellurium co-precipitation. *J. Anal. At. Spectrom.* 15, 747–751, doi: [10.1039/b000470g](https://doi.org/10.1039/b000470g).
- Kholodov, V.N., Nedumov, R.I., 2005. Application of the molybdenum module for reconstruction of the gas composition of water in the Cretaceous Atlantic. *Dokl. Earth Sci.* 400 (1), 116–118.
- Kizil'shtein, L.Ya., 2000. The role of organic matter in the formation of gold deposits (by the example of black shales). *Rossiiskii Khimicheskii Zhurnal* 44 (3), 108–114.
- Kolesnik, A.N., Kolesnik, O.N., Karabtsov, A.A., Bondarchuk, N.V., 2018. Mineral grains of base and precious metals in the surface layer of bottom sediments in the Chukchi Sea. *Dokl. Earth Sci.* 481, 887–892, doi: [10.1134/S1028334X18070085](https://doi.org/10.1134/S1028334X18070085).
- Kolesnik, A.N., Selyutin, S.A., Kolesnik, O.N., Bosin, A.A., Astakhov, A.S., Vologina, E.G., Sukhoveev, E.N., Bazhenov, I.I., 2023a. An efficient approach to the sequence stratigraphic study of monotonous Holocene sediments from the Arctic Shelf. *Dokl. Earth Sci.* 512, 1024–1031, doi: [10.1134/S1028334X23601384](https://doi.org/10.1134/S1028334X23601384).
- Kolesnik, O.N., Kolesnik, A.N., Astakhov, A.S., 2023b. Geochemistry and mineralogy of rare-earth elements in ferruginous deposits and bottom sediments of the Laptev Sea. *Russ. Geol. Geophys.*, doi: [10.2113/RGG20234491](https://doi.org/10.2113/RGG20234491).
- Kubrakova, I.V., Fortygin, A.V., Lobov, S.G., Koshcheeva, I.Ya., Tyutyunnik, O.A., Mironenko, M.V., 2011. Migration of platinum, palladium, and gold in the water systems of platinum deposits. *Geochem. Int.* 49, 1072–1084, doi: [10.1134/S0016702911110061](https://doi.org/10.1134/S0016702911110061).
- Kubrakova, I.V., Nikulin, A.V., Koshcheeva, I.Ya., Tyutyunnik, O.A., 2012. Platinum metals in the environment: Content, determination, behaviour in natural systems. *Chem. Sustainable Dev.* 20 (6), 593–603.
- Kubrakova, I.V., Tyutyunnik, O.A., Koshcheeva, I.Ya., Nabiullina, S.N., Sadagov, A.Yu., 2017. Migration behavior of platinum group elements in natural and technogeneous systems. *Geochem. Int.* 55, 108–124, doi: [10.1134/S0016702916120053](https://doi.org/10.1134/S0016702916120053).
- Kubrakova, I.V., Nabiullina, S.N., Pryazhnikov, D.V., Kiseleva, M.S., 2022. Organic matter as a forming and transporting agent in transfer processes of PGE and gold. *Geochem. Int.* 60, 748–756, doi: [10.1134/s0016702922080031](https://doi.org/10.1134/s0016702922080031).
- Kutyrev, A.V., Bundtzen, T.K., Sidorov, E.G., Chubarov, V.M., 2020. Placer platinum of the Bub Creek and its significance for the classification of ultrabasic rocks of Alaska, in: Under the Sign of Gold and Platinum. Ural Mineralogical School 2020. Proceedings of the 26th All-Russian Scientific Conference with International Participants [in Russian]. Al'fa Print, Yekaterinburg, pp. 56–58.
- Li, L., Liu, Y., Wang, X., Hu, L., Yang, G., Wang, H., Bosin, A.A., Astakhov, A.S., Shi, X., 2020. Early diagenesis and accumulation of redox-sensitive elements in East Siberian Arctic Shelves. *Mar. Geol.* 429, 106309, doi: [10.1016/j.margeo.2020.106309](https://doi.org/10.1016/j.margeo.2020.106309).
- Lisitsyn, A.P., 1966. Processes of Recent Sedimentation in the Bering Sea [in Russian]. Nauka, Moscow.
- Logvinenko, N.V., Ogorodnikov, V.I., 1980. Recent bottom sediments of the Chukchi Sea shelf. *Okeanologiya* 20 (4), 681–687.
- Matveeva, T., Savvichev, A., Semenova, A., Logvina, E., Kolesnik, A., Bosin, A., 2015. Source, origin, and spatial distribution of shallow sediment methane in the Chukchi Sea. *Oceanography* 28, 202–217, doi: [10.5670/oceanog.2015.66](https://doi.org/10.5670/oceanog.2015.66).
- Nesterenko, G.V., Kolpakov, V.V., Boboshko, L.P., 2014. Native gold in sedimentary cycle: notes on the problem in the light of the F.N. Shakhov statement, in: Noble, Trace, and Radioactive Elements in Ore-Forming Systems. Proceedings of the All-Russian Conference with International Participants [in Russian]. INGG SO RAN, Novosibirsk, pp. 506–512.
- Pashkova, E.A., Danilova, E.A., Lyutsarev, S.V., Levitan, M.A., 1988. Gold and organic matter in the Holocene deposits of the Bering Sea. *Litologiya i Poleznye Iskopaemye* 23 (5), 101–109.
- Pavlidis, Yu.A., 1982. Depositional environment in the Chukchi Sea and facies–sedimentation zones of its shelf, in: Problems of Shelf Geomorphology, Lithology, and Lithodynamics [in Russian]. Nauka, Moscow, pp. 47–76.
- Reimer, P., Baillie, M.G.I., Bard, E., Bayliss, A., Beck, J.W., Blackwell, P.G., Bronk Ramsey, C., Buck, C.E., Burr, G.S., Edwards, R.L., Friedrich, M., Grootes, P.M., Guilderson, T.P., Hajdas, I., Heaton, T.J., Hogg, A.G., Hughen, K.A., Kaiser, K.F., Kromer, B., McCormac, F.G., Manning, S.W., Reimer, R.W., Richards, D.A., Southon, J.R., Talamo, S., Turney, C.S.M., van der Plicht, J., Weyhenmeyer, C.F., 2009. IntCal09 and Marine09 radiocarbon age calibration curves, 0–50,000 years cal BP. *Radiocarbon* 51, 1111–1150, doi: [10.1017/S0033822200034202](https://doi.org/10.1017/S0033822200034202).
- Scholz, F., Siebert, C., Dale, A.W., Frank, M., 2017. Intense molybdenum accumulation in sediments underneath a nitrogenous water column and implications for the reconstruction of paleo-redox condi-

- tions based on molybdenum isotopes. *Geochim. Cosmochim. Acta* 213, 400–417, doi: [10.1016/j.gca.2017.06.048](https://doi.org/10.1016/j.gca.2017.06.048).
- Sklyarov, E.V. (Ed.), 2001. Interpretation of Geochemical Data [in Russian]. Internet Inzhiniring, Moscow.
- Tissot, B., Welte, D.H., 1978. Petroleum Formation and Occurrence: A New Approach to Oil and Gas Exploration. Springer-Verlag, Berlin, doi: [10.1007/978-3-642-96446-6](https://doi.org/10.1007/978-3-642-96446-6).
- Tsar'kova, P.A., Biryukova, M.V., Lazareva, E.V., Pertsov, N.V., 1993. A technique for the fractionation of marine sediments of a shelf zone for detecting finely dispersed gold. *Geokhimiya*, No. 6, 879–881.
- Tsoy, I.B., Obrezkova, M.S., Aksentov, K.I., Kolesnik, A.N., Panov, V.S., 2017. Late Holocene environmental changes in the Southwestern Chukchi Sea inferred from diatom analysis. *Russ. J. Mar. Biol.* 43, 276–285, doi: [10.1134/S1063074017040113](https://doi.org/10.1134/S1063074017040113).
- Varshall, G.M., Velyukhanova, T.K., Baranova, N.N., Koshcheeva, I. Ya., Shumskaya, T.V., Kholin, Yu.V., 1994. Formation of silver complexes with humic acids and the geochemical role of this process. *Geokhimiya*, Nos. 8–9, 1287–1294.
- Vologina, E.G., Sturm, M., Kulagina, N.V., Aksentov, K.I., 2023. Composition of Late Holocene deposits in the southern Chukchi Sea. *Oceanology*, 74–83, doi: [10.1134/S0001437023010162](https://doi.org/10.1134/S0001437023010162).
- Wentworth, C.K., 1922. A scale of grade and class terms for clastic sediments. *J. Geol.* 30 (5), 377–392, doi: [10.1086/622910](https://doi.org/10.1086/622910).
- Yudovich, Ya.E., Ketris, M.P., 1988. Geochemistry of Black Shales [in Russian]. Nauka, Leningrad.